3D Printed Soft and Flexible Insole With Intrinsic Pressure Sensing Capability

M. Ntagios, *Member, IEEE*, and Ravinder Dahiya, *Fellow, IEEE*

***Abstract*—This work presents a soft, flexible, and low-cost capacitive pressure-sensitive insole developed using resource-efficient single-step 3D printing method. Developed using elastomeric materials, the soft and robust sensory insole can bend and twist in extreme angles. The insole is designed to have four sensing zones to capture the pressure information from the entire contact area. The sensors tested under different condition of applied pressure showed reliable response up to 300kPa without saturation. The sensors exhibit a sensitivity of 2.4MPa^{-1}for range of 0 - 60kPa and 0.526MPa^{-1} for 60kPa and above with average sensitivity of 1.314 MPa^{-1} in the entire range. The insole was also tested under varying bending and temperature conditions. Considering the excellent response over a wide pressure range, the presented insole could be used for gait analysis or with anthropomorphic robots for critical information about the terrain morphology. To show the functionality of presented insole, we have also developed an app to display the sensory information obtained via custom-made electronics circuit.**

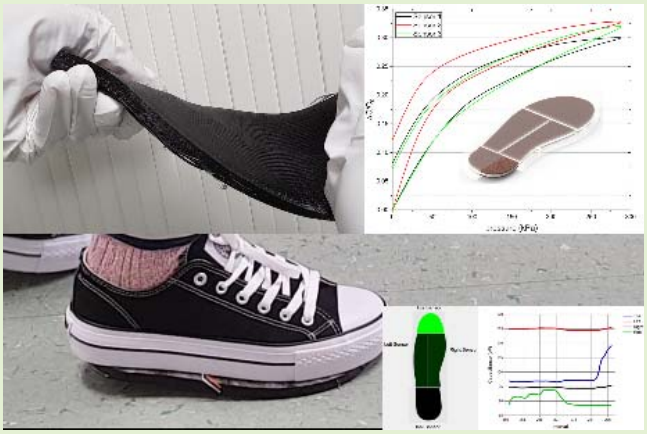

***Index Terms*—3D printing, additive manufacturing, pressure sensors, tactile sensors, robotics, wearable electronics.**

I. Introduction

ROBOTIC systems have evolved in the recent years with improved control algorithms and wide range of distributed sensors, actuators and energy devices etc. [1]. Using the advanced sensing technologies with motion capture suits, the engineers are now able to use anthropomorphic robots to replicate complex human-like movements such as dancing [2], [3]. These advancements have provided robots an ability to perform highly agile manoeuvres that even humans would find it challenging such as backflips or jumping [4], [5]. However, many of these advancements have been demonstrated in structured environments where engineers and researchers have absolute control. Once these systems are placed in an unstructured terrain with uneven surfaces, they are likely to struggle to replicate even the simplest of task such as standing up right [6]. The reason for this, is the lack of information about the terrain they are standing or walking on. Information such as material softness/hardness, surface morphology/topology and pressure applied in different areas of the foot are critical for succeeding in walking/running in difficult terrain such as mines, forests, hill sites etc.

To address the need for pressure sensing feedback in robotics, a wide variety of tactile or pressure sensors have been reported [7]–[11]. Although some of these sensors have been used for feedback during tasks such as walking, a vast majority of them (pressure [12]–[14], temperature [15] or proximity [11], [16]) have been mainly developed for e-skin robotic systems and as wearables where expected pressure ranges are not too high [17]–[19]. For example, normal manipulation involves forces in the range of 15–90 gm. wt. and 90% of the mechanoreceptors can detect forces as low as 85 mN [20]. Most of the sensors developed for e-skins saturate or fail to withstand large body weight. As a result, the need for sensorised insole in legged robots, to obtain touch or pressure feedback from foot, is not fully met. Several factors that may have contributed to this gap include fragility of materials, difficulty in terms of scalability, wiring, and high cost of materials and the fabrication processes. Some of the current approaches rely on using off-the-shelf sensors [21]–[23],

Manuscript received 9 April 2022; revised 18 May 2022; accepted 18 May 2022. Date of publication 10 June 2022; date of current version 16 October 2023. This work was supported in part by the Engineering and Physical Sciences Research Council (EPSRC) through Engineering Fellowship for Growth—neuPRINTSKIN under Grant EPR/R029644/1, in part by the National Productivity Investment Fund under Grant EP/R512266/1, and in part by Shadow Robot Company Ltd., U.K. The associate editor coordinating the review of this article and approving it for publication was Prof. Huang Chen Lee. *(Corresponding author: Ravinder Dahiya.)*

The authors are with the Bendable Electronics and Sensing Technologies (BEST) Group, University of Glasgow, Glasgow G12 8QQ, U.K. (e-mail: ravinder.dahiya@glasgow.ac.uk).

This article has supplementary downloadable material available at https://doi.org/10.1109/JSEN.2022.3179233, provided by the authors.

Digital Object Identifier 10.1109/JSEN.2022.3179233

which often limits the topology of the sensing area to specific regions of the insole with wires exposed to the external area of the foot/insole. Other works include sensors using modalities such as piezoresistive sensors, capacitive sensors or optical sensors [8], [24]–[32].

Capacitive sensor configuration is preferred here over resistive sensors as they respond to a larger force before saturating, they require lesser power and need simple front-end electronics. Resistive sensors generally have a hyperbolic response which could be better for low pressure measurements [9]. Further, the response of resistive structures could be considerably influenced by bending of structure. Recently, parallel plate capacitive sensors have been reported using conductive textile and non-conductive rubber as a dielectric [33]. Sensors with textile composites (e.g., nylon-filter-paper-based multiwall carbon nanotubes and poly(3,4-ethylenedioxythiophene) polystyrene sulfonate MWNT/PEDOT:PSS) as electrodes and porous Polydimethylsiloxane (PDMS) as a dielectric have also been reported. [34]. These sensors show low sensitivity and they are difficult to integrate or use in a wearable structures. Further, often these devices are realized using complex and resource inefficient manufacturing processes such as photolithography, etching etc. and they do not meet the need for a low-cost soft, flexible and robust tactile/pressure sensors. In this regards, additive manufacturing or 3D printing could be used.

Recent advances in 3D printing show that it has evolved from a simple tool that hobbyists use for decorative purpose to one that allow complex shapes with embedded sensing and electronic functionalities. Many new devices have been fabricated using this technology with factional purpose [35] for medical application (e.g. prosthodontics, implants), aerospace with spacecraft brackets, robotics with 3D printed robotic hands and sensors and electronics with 3D printed antennas, interconnects, and storage devices etc. [36]–[44]. 3D printing enables the fabrication of devices that could not be fabricated with different techniques, enables fast prototyping and reduces the cost of production with minimal material waste something that is being proven extremely important in the initial stage of the Covid-19 pandemic with 3D printed protective gear and ventilators [45], [46]. Additive Manufacturing is also attractive in terms of circular economy, a crucial component for sustainable future [47].

In this work, we present a 3D printed capacitive pressure-sensitive insole for anthropomorphic robots. The devices were fabricated using direct multimaterial 3D printing, which provides substantial advantages in terms of design flexibility, dimensional control and the automation. In contrast, other sensors are fabricated using methods involving several steps and/or manual assembly [48], [49]. Many tactile sensors reported so far are bulky and come in predefined shape leaving little room for design flexibility. In this regard, the 3D printed sensor approach presented in this paper is distinct as it allows formation of the entire sensor structure by printing, which is easily reproducible, and design changes can be quickly implemented. In addition, 3D printing also provides an opportunity to encapsulate other devices such as energy harvesters [50]. The fabricated device provides pressure data to the user via the four fully embedded capacitive pressure sensors. The insole has sensors placed in such a way that they cover the entire area of the foot. The sensors placements ensure that the foot is capable of withstanding large pressure and is also able to bend or twist as needed during walking. The work presented in this paper is extends the preliminary results presented in IEEE FLEPS 2021 [33]. The new results here include results based on fabrication of new devices, their extensive characterization with much wider range of applied forces (up to 1000N), bending and temperature response, as well as, time response of the devices and the real-time method of capturing the response of the devices and presenting them to a Personal Computer (PC).

The paper is organized as follows: Section II describes the design of the sensorised insole and presents the fabrication process. Section III presents the characterization results of all the experiments that have been conducted. Section IV presents the integration and demonstration of one of the insoles in a real condition environment and finally the Section V summarizes the key findings of this work and comparisons with the existing literature.

II. Design & Fabrication of Sensorised Insole

A. Design of Sensorised Insole

The device was designed to resemble a human foot using state-of-the-art Computer-Aid-Design (CAD) software. The software used was SolidWorks 2017 (SOLID Applications Limited) for drawing the design. The size of the insole resembles a size 4 UK shoe. The limiting factor to the insole design was the build area of the used 3D printer (Ultimaker S5). The insole's design was done to accommodate four embedded pressure sensors to cover the entire insole area. The four sensors are capacitive pressure sensors fabricated with two different techniques - 3D printing and drop-casting. A total of 8 holes are designed at the side of each capacitive plate, for the wire bonding, while the device was entirely fabricated using the 3D printer without the need of any other fabrication tool.

The insole is 225mm long from heel to toe, from side to side it is 87 mm long and the thickness is 10.5mm. Each electrode has thickness of 1.4mm and the dielectric has thickness of 4mm. The toe sensor covers an area of 3,356 mm^2, the left and right sensors cover an area of 2,855 mm^2 and 2,482 mm^2 respectively and the heel sensor covers about 2,100 mm^2. Fig. 1 presents the design and dimensions of the sensorised insole for anthropomorphic robotic systems.

The operating principle of the sensor is based on a parallel plate configuration. The two parallel conductive plates are separated by a distance d_1 with a dielectric material in between with a dielectric constant of ε. The equation to calculate the capacitance of the structure is $C = \varepsilon^*A/d$. Once a force is presented on the top of the structure the distance between the plates is decreasing (d_2) resulting in the increase of the capacitance.

B. Fabrication

The pressure sensitive insole was developed using a multimaterial 3D printing system. The capacitive sensors are 3D

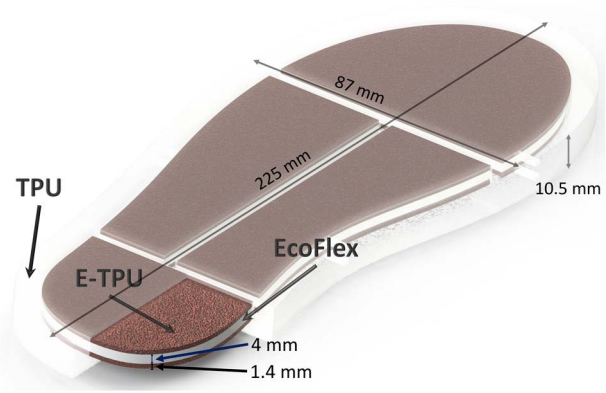

Fig. 1. X-Ray view of the sensorised pressure sensor insole for anthropomorphic robotics.

printed using the Ultimaker S5, a 3D printer capable of printing two materials in the same print. The first material was a Thermoplastic Polyurethane (TPU) filament (NinjaFlex, NinjaTek) mounted on the first nozzle of the printer. The second was a conductive thermoplastic filament, PI-ETPU (Palmiga-PI-ETPU 95-250 Carbon Black). The PI-ETPU filament was used to fabricate the electrodes of the capacitive sensors and the TPU was used as an encapsulation material for the sensors. Ecoflex 00-30 (Smooth-On) was used in 1:1 ratio to form the dielectric layer of the capacitive sensors.

The printer was mounted with two 0.4mm nozzles with the TPU material attached to the first nozzle and the PI-ETPU on the second nozzle. The slicer software used was Cura 4.7.1 (Ultimaker). The optimized printing parameters and the materials used are as follows. The layer height was 0.2mm, speed was set to 25 mm/s for both materials, the printed temperature for the TPU was set to 240 ^{o}C and 250 ^{o}C for the PI-ETPU and the temperature of the bed was set to 45 ^{o}C. The infill for the TPU was set to 85% and for the PI-TPU was set to 95%. The file that generated the instruction for the printer (gcode) was created using Cura and was modified to include pauses at layers 21, 38, 41. The total time for printing one device was about 18 hours on average.

Initially, the print started with the deposition of TPU on the bed of the printer. The printer at layer 18 started the deposition of the bottom electrodes. At layer 21, the printer was paused to allow access to the bottom electrodes for wire bonding. Thin wires were placed on top of the electrodes and a small amount of silver paint (RS Pro Silver Conductive RS186-3600, RS Components) was applied on top of the area where the wire and the electrode were touching, to reduce the conduct resistance, and left for some time to allow it to dry. Fig. 2b show the result of this process. Once the wires were secured and the paint dried, the printing process was resumed. At layer 38, the printer was paused again to form a cavity with depth equal to the thickness of the dielectric. Once the printer was paused, the material needed for the soft dielectric layer between the two printed electrodes of capacitor was prepared. For this, the Ecoflex was prepared separately in a beaker, and it was poured at 1:1 weight ratio, then part A and part B were mixed rigorously for about 20 minutes. After this the beaker was placed under vacuum for about 10 minutes to remove all bubbles from the mixture. After, the mixture was removed from the vacuum, it was drop casted on the cavities of the capacitive sensors to form the dielectric layer. The excess amount of material was removed by scraping the entire device leaving an even level plane with the rest of the print. Alternatively, the dielectric layer can also be 3D printed using methods such as Direct Ink Writing. The device was left to cure for about an hour. Once the dielectric was completely cured the area of the dielectric was covered with a thin masking tape (RS Pro 60° paper masking tape, RS Components). This is due to poor adhesion of PI-ETPU with Ecoflex as direct deposition of PI-ETPU was found to be challenging. Once the process was completed, the print resumed until layer 41. Once the printer reached that layer the system was paused, and the wire bonding of the top electrodes was carried out (Fig. 2i). The same process was followed as the bottom electrodes for wire bonding. After this the printing of the last layers of the device was carried out. The outcome of this fabrication process was a flexible, soft, and highly bendable structure that can be seen in Fig. 3a-b. The 85% infill of the TPU material allows the structure to be softer than a 100% solid TPU structure. This makes it more attractive for wearable applications such as in walk monitoring systems as it absorbs impact more gradually than a solid block.

III. Characterization of Sensing Insole

Three separate insoles were fabricated for characterization. From those three fabricated insoles, the toe sensors were characterized and compared with each other under three different testing conditions. The first set of experiments was to determine the response of the sensors with respect to the applied pressure. Secondly, they have been tested for a prolonged cycling response, to confirm the reliability and robustness of the sensor during actual use when frequent force is expected. Lastly, the devices were tested for their time response.

The capacitive transducers were characterized for their response with respect to different magnitude of force. The devices were tested under increasing and decreasing amount of the applied pressure. The toe sensors were tested under extreme loads. All sensors were tested up to 300kPa pressure with a step of 30kPa. This covers a much wider range of forces than the devices may experience during use. Even at extreme pressures, the sensors did not alter their functionality. Fig. 4 presents the relative change of capacitance with respect to the applied pressure for all three devices. It can be observed that there are two linear regimes of the sensors' response. The first linear region is from 0 - 60kPa with sensitivity of 2.4 MPa^{-1}. The second range is from 60kPa to 300kPa, for which the sensitivity was found to be 0.526MPa^{-1}. The sensors exhibit an average maximum hysteresis of 9.57%. The highly sensitive range is due to the deformation of the softer elastomer (e.g., dielectric material). The second range is mostly due to the deformation of the encapsulation material. The TPU material, that encapsulates the transducer, can deform at a different rate from the softer elastomer. Thus, the transducers do not saturate at low forces, extending the measuring range of the device.

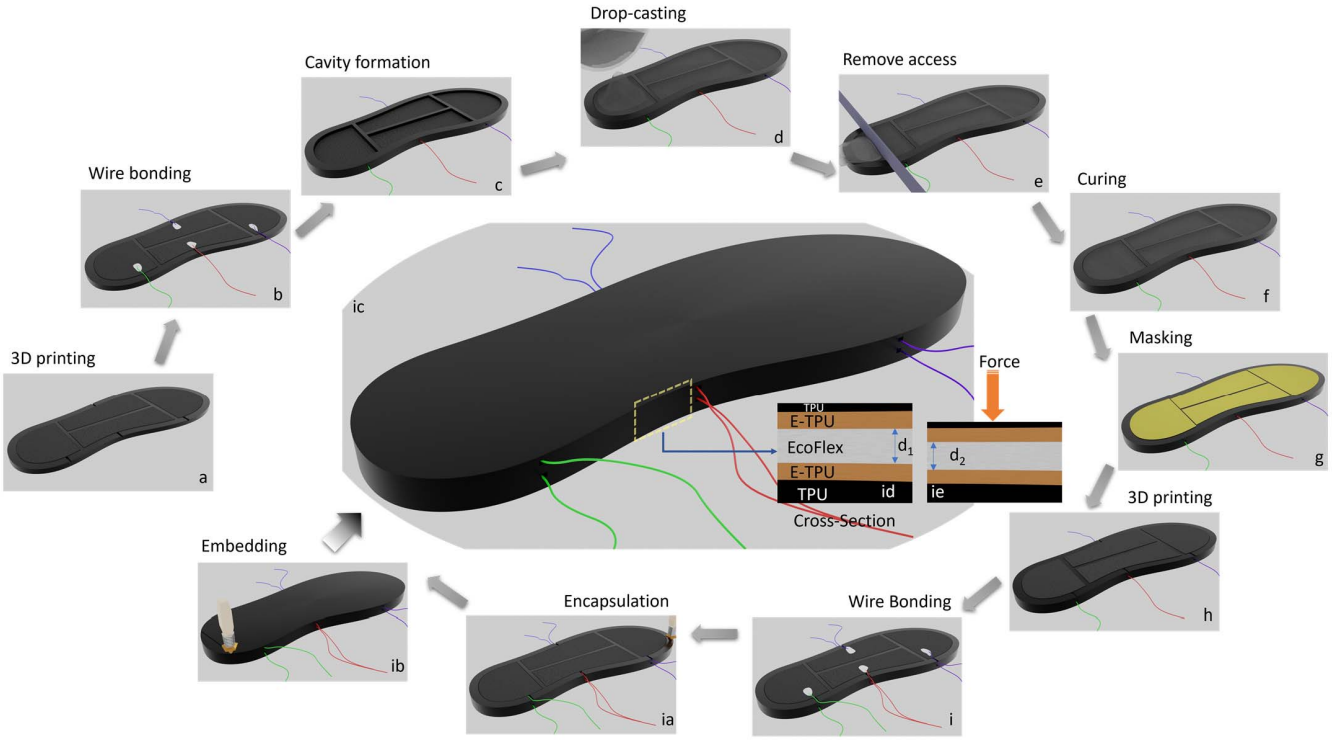

Fig. 2. Fabrication process of the 3D printed embedded capacitive pressure sensors insole. a-ib) Fabrication steps for 3D printing the insole. ic) final depiction of the pressure sensing device. id) Cross-Section presenting the different materials under no applied force. Ie) Cross-Section view of the structure with applied force.

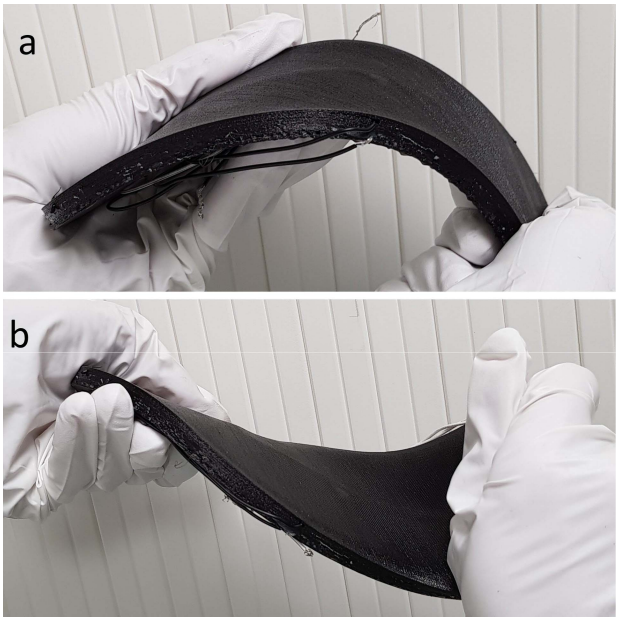

Fig. 3. a) Fabricated 3d printed capacitive pressure insole under bending condition. b) Sensorised insole viewed while twisted.

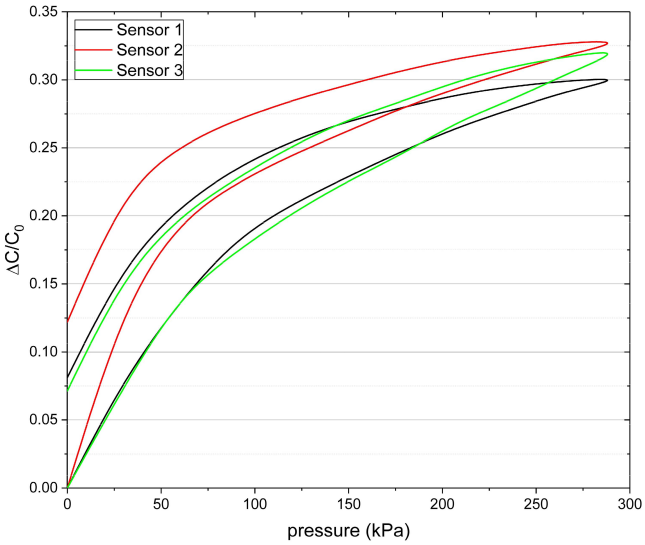

Fig. 4. Relative change of capacitance with respect to pressure of the three-3D printed capacitive tactile sensors insoles.

Next, the three sensors were tested for long-term stability of the response. All sensors were applied with pressure of 30kPa for 1000 cycles. Each device was tested for 2 hours and 46 minutes and each cycle lasted for 5 seconds of applied force followed by 5 seconds relaxed state i.e., no force applied. Fig. 5 presents the relative change of capacitance for each cycle for all three sensors. All three devices have similar responses with some deviation change from cycle to the next cycle. This deviation presents a percentage deviation of 8.5% of the relative change of capacitance. Nevertheless, it can provide the necessary tactile information for potential use of tactile sensing in robotic application where pressure information is needed during prolonged use in harsh terrains.

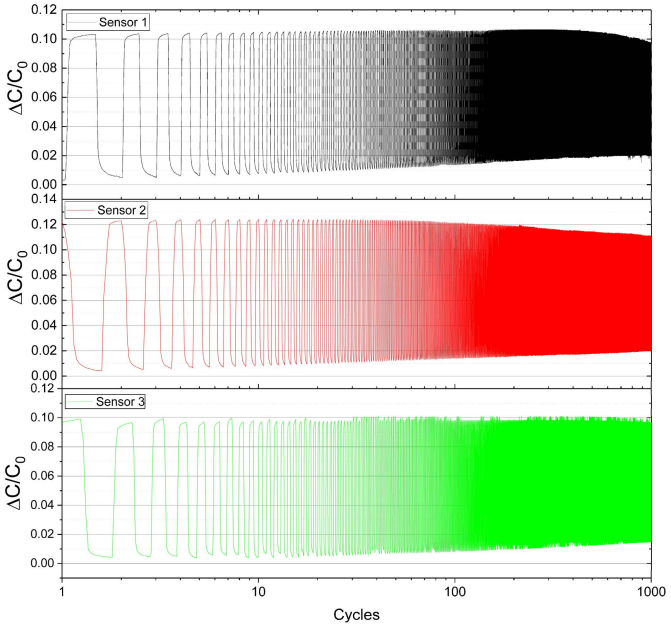

Fig. 5. Cyclic performance of three devices for 1000 cycles at 30kPa of pressure.

TABLE I
TIME RESPONSE OF 3D PRINTED INSOLE

Direction	Time to reach 90% (s)	Time to reach 98%(s)
Increasing force	3.2	107
Decreasing force	25.5	170

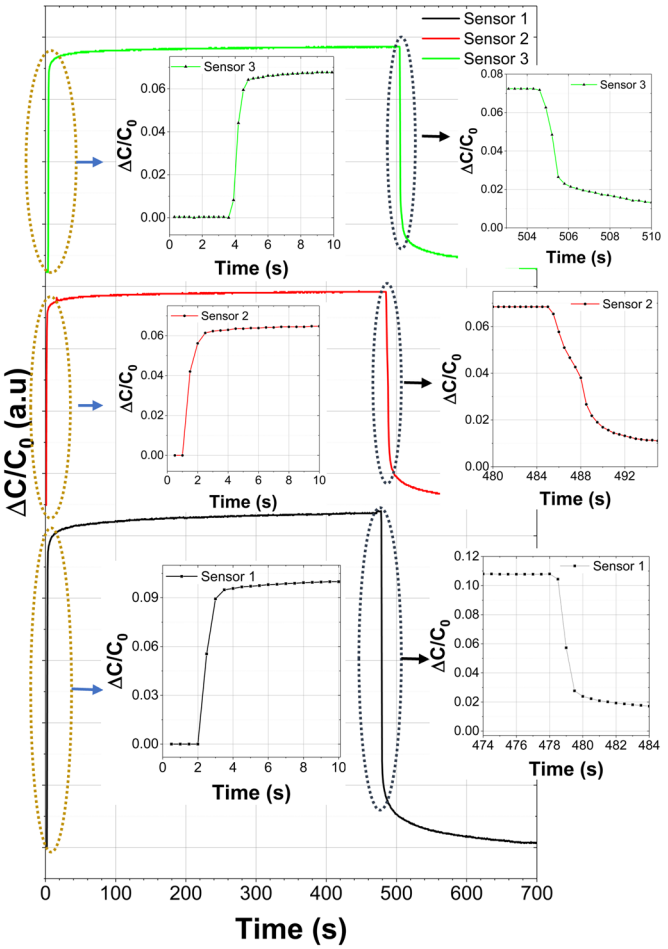

Fig. 6. Response of the 3D printed insole over time with a sudden increase and decrease of the load.

Last set of experimentation was to see the time it takes for the sensors to respond to the changes in applied force. The sensors at the beginning were not under any stress. Then a load of 20kPa was applied for a long period. The capacitance of the device was continuously measured. Once the sensor had a constant (or saturated) response, the applied force was suddenly removed to measure the response time. Fig. 6 presents the results of the measurements. All devices had similar response. The average response time of the sensors to reach 90% of the applied force value was found to be 3 seconds and the time to reach 98% was slightly over 1 min. For decreasing load, the sensors average time response from 0 to 90% was found to be 25.5 seconds with a total of 2 minutes to reach the 98%. Table I summarizes the results of the experimentation. The difference in response times at the time of application for force and its removal, is likely due to the viscoelastic effect of the Ecoflex resulting in an increase time response of the device when forces are released. The time response of the device is somewhat large compared to other sensors reported in the literature this is due to the ecapsulation material (TPU) and dielectric material (Ecoflex) as elastomeric materials resist deformation. This drawback is due to the large thickness of the overall structure. This affect can be minimized with decreasing the overall thickness of the device.

To further evaluate the 3D printed capacitive sensing insole, all sensors in it were characterized under different conditions. Two sets of experiments were conducted: The first was to characterize the sensors with respect to applied pressure up to maximum load of 1000N. As the surface area of each sensor differs slightly, the coresponding pressure response for each sensor differs as well. The response of the sensors from one insole is given in Fig. 7. The right sensor exhibits sensitivity of 0.854 MPa^{-1} for the entire pressure range while the left section exhibits sensitivity of 1.065 MPa^{-1} and the heel sensor's sensitivity is 0.867 MPa^{-1}.

Furthermore, the device was tested under different bending conditions and the response of each sensor was recorded. In this experiment one of the insole was placed in such a way that only the front and back of the device were touching the test set up, as shown in the inset in Fig. 8. A linear motor was placed above the centre of the device and was able to bend the device at specific intervals. The maximum bending curvature that the device experienced was 5.6 m^{-1}. Fig. 8 shows the relative change of capacitance with respect to bending curvature. All sensors exhibited linear response. The sensitivities for the right and the left sensors were 0.0133m and 0.0143m respectively. The toe and the heel sensors exhibited a lower sensitivity of 0.003m and 0.006m, respectively. The different sensitivities of these sensors are due

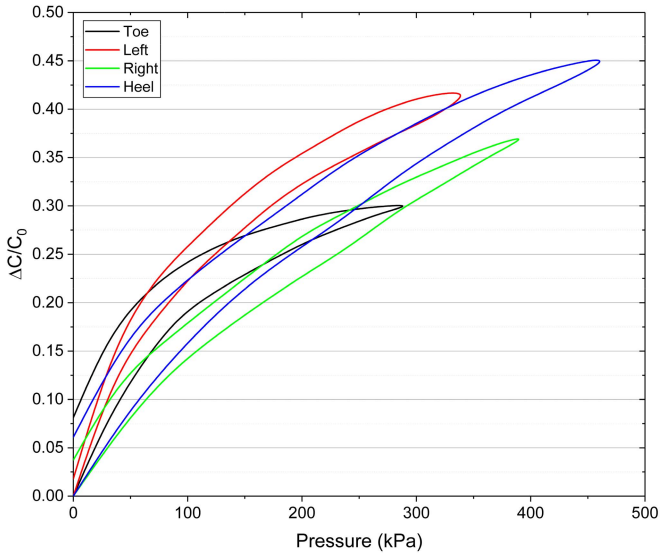

Fig. 7. Relative change of capacitance with respect to pressure for all four sensors in one of the 3D printed insole.

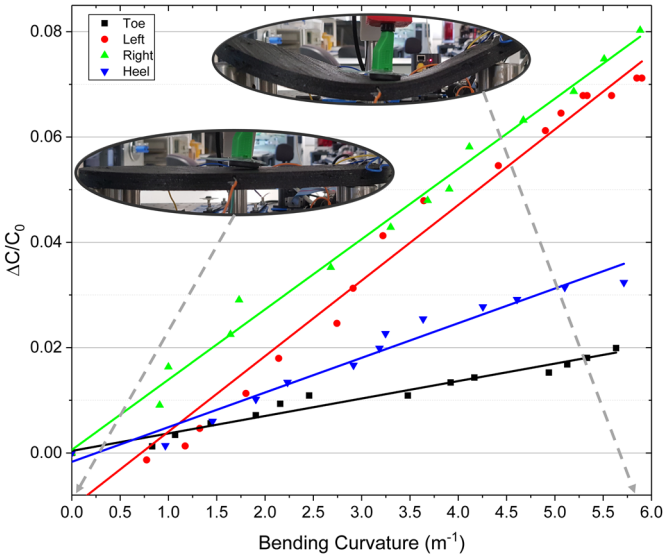

Fig. 8. Relative change of capacitance with respect to bending curvature for all four sensors in one of the 3D printed capacitive sensing devices.

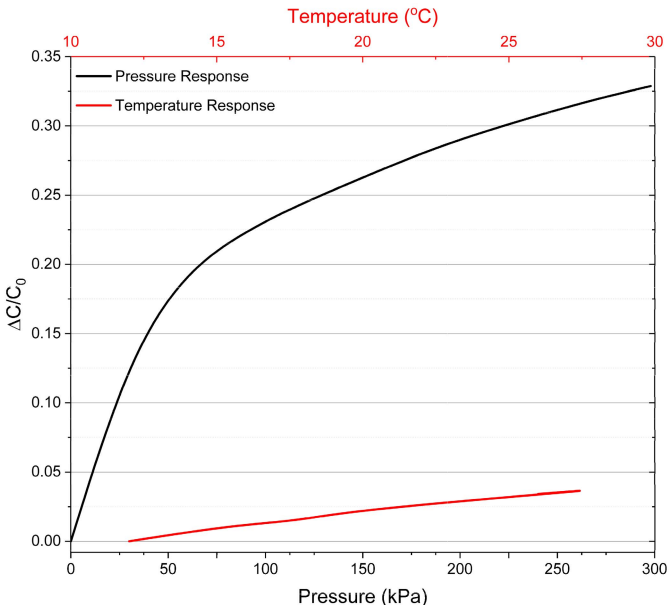

Fig. 9. Relative change of capacitance with respect to temperature and pressure of the toe sensor.

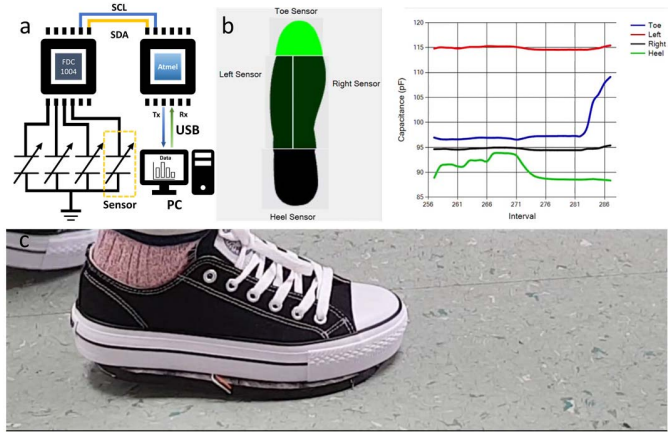

Fig. 10. Demonstration of 3D printed insole under load. a) electronic circuit schematic of the system. b) GUI created to represent the data received from the microcontroller. c) sensorised insole under load and connected to external electronics for capacitive measurement.

to the geometrical/dimensional differences, as the sensors in the centre are longer than the ones at heel and toe.

The 3D printed insole was also tested under different temperatures to observe the potential response variation in outdoor conditions. The device was at first left overnight in a cold environment at a temperature of 11 °C and then was placed at room temperature (23 °C) and the output of the toe sensor was monitored with an infrared non-contact digital thermometer. The temperature and capacitance of the device was monitored constantly and logged. Once the device reached room temperature, a heat gun was placed above the device at a 30 cm distance and it was set to 100 °C at maximum air flow. The device started to heat and the temperature and response of the sensor were continuously monitored. The maximum temperature the device experienced was 29 °C. Fig. 9 shows the relative change of capacitance with respect to temperature and at the same time the response to pressure for comparison. The sensor shows a liner response with temperature with a sensitivity of 0.0023 $°C^{-1}$. This shows that the relative change in capacitance due to temperature variation of 18 °C is equivalent to the 15kPa of applied pressure.

Table II compares this work with respect to other similar works reported in the literature. From the table is clear the sensors in the 3D printed insole provide a higher sensitivity than the most works reported in the literature.

IV. Demonstration

Once the device characterization was completed, one of the tested devices was further used to demonstrate the capabilities of presented approach in application such as sensory feedback during walking. For this, the device was integrated with a

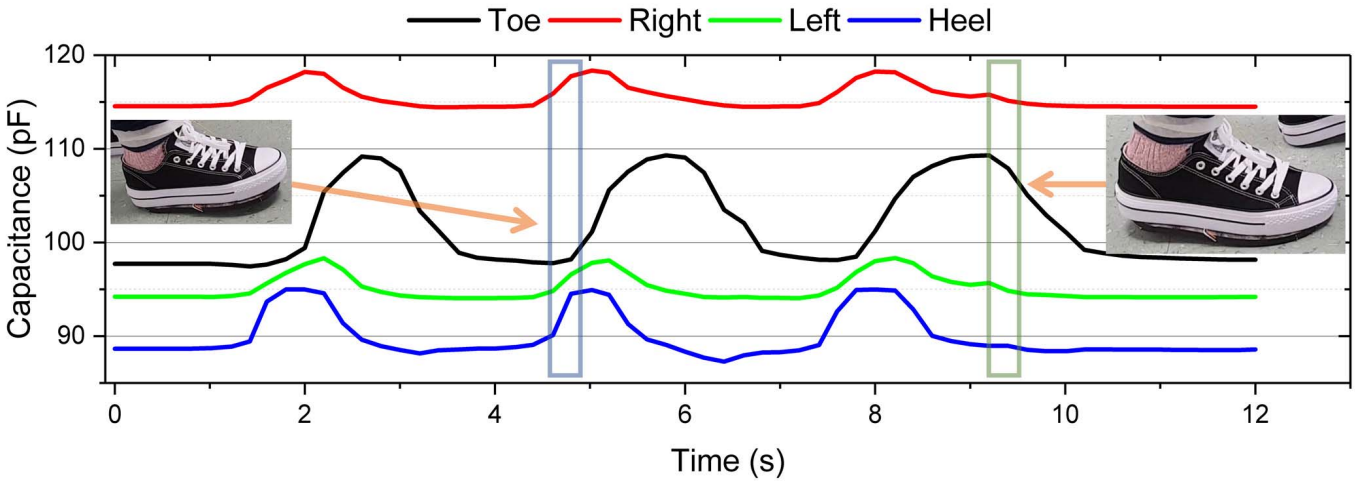

Fig. 11. Shoe integrated with the 3D printed embedded capacitive sensorised insole used for gait analysis, presenting the data capture from the MCU in real-time over three steps of the right leg.

TABLE II
COMPARISON OF 3D PRINTED INSOLE WITH PREVIOUS WORKS

Materials	Sensitivity	Range	3D printed?	Ref.
Gold thin films-Silicone rubber	0.4 MPa^{-1}	160kPa	No	[51]
MWNT/PEDOT:PSS-Porous PDMS	1.12 MPa^{-1}	1400kPa	No	[34]
Conductive PDMS-Ecoflex	0.42 MPa^{-1}	1200kPa	Yes	[52]
Gold-Ecoflex	0.48 MPa^{-1}	250kPa	No	[53]
Silver cloth-cotton cloth	0.95 MPa^{-1}	200kPa	No	[49]
ETPU-Ecoflex	**1.31 MPa^{-1}**	300kPa	Yes	This Work

Capacitive-to-Digital Converter (CDC) Integrated Circuit (IC) chip (FDC1004-4, Texas Instruments). The IC was connected to a microcontroller (Atmel SAM3 × 8E ARM Cortex-M3) (MCU) using Inter-Integrated Circuit (I^2C) communication protocol and the microcontroller was connected to a Personal Computer (PC) via Universal Serial Bus (USB) connector (Fig. 10a). A custom-made C-sharp program was made to represent the data captured from the IC as a Graphical User Interface (GUI). The GUI presents the data in two ways.

The GUI on the top left side of the screen has an insole shape image segmented in four parts that represent the area of the respected sensor. At the start, the image area is black and represents no pressure applied to the specific sensor. As pressure increases, the pressed part of the insole starts to become green and with an increase in pressure the intensity of the green colour further increases. On the right is the graph displaying the capacitance for each sensor. The graph updates in real-time thus providing a better understanding of the history of each sensors' response. Fig. 10b shows the GUI of the system. Fig. 10c is a snapshot of the device being pressured upon and the response is provided via the GUI. Support Video I show the working of the presented insole and the real-time data transfer to the user for further use such as using feedback for stable standing of a robot.

The device was also tested for gait analysis. The sensorized insole was securely placed under a shoe and the wearer walked at a normal pace. The realitime data captured with GUI for three steps of the right leg is shown in Fig. 11. Support Video II show the experement for the gait analysis. From the data we can clearly see the walking patern of the individual and can see the repeatability of the response.

V. CONCLUSION

Here in, we presented a novel sensorised insole for potential use in anthropomorphic robotic systems and beyond where extreme load conditions are expected during walking or standing, and sensory feedback is critical. The sensorised insole was developed using multimaterial 3D printing approach. This approach is attractive due to ease of customization, simplicity of manufacturing, bendability, low-cost, durability, and resource efficiency. The sensors were tested for loads up to 1000 N, which is equivalent of the load experienced with an above average male adult standing on one leg and on his toe. The sensor provides two linear response ranges from 0 to 60kPa and from 60 kPa to 300kPa. This approach can be used not only for robotic systems but also in wearables to monitor performance of athletes and heath/rehabilitation applications. Further, the approach could be extended to print insole and similar smart structures with intrinsic devices for functionalities such as energy harvesting and storage.

REFERENCES

[1] R. Mukherjee, P. Ganguly, and R. Dahiya, "Bioinspired distributed energy in robotics and enabling technologies," *Adv. Intell. Syst.*, May 2021, Art. no. 2100036, doi: 10.1002/aisy.202100036.
[2] E. Guizzo, "By leaps and bounds: An exclusive look at how Boston dynamics is redefining robot agility," *IEEE Spectr.*, vol. 56, no. 12, pp. 34–39, Dec. 2019, doi: 10.1109/MSPEC.2019.8913831.
[3] R. Chirila, M. Ntagios, and R. Dahiya, "3D printed wearable exoskeleton human-machine interfacing device," in *Proc. IEEE SENSORS*, Oct. 2020, pp. 1–4, doi: 10.1109/SENSORS47125.2020.9278611.
[4] Boston Dynamics. *ATLASTM*. Accessed: Sep. 23, 2021. [Online]. Available: https://www.bostondynamics.com/atlas
[5] A. Goswami and P. Vadakkepat, *Humanoid Robotics: A Reference*. Dordrecht, The Netherlands: Springer, 2019.
[6] G. Wiedebach *et al.*, "Walking on partial footholds including line contacts with the humanoid robot atlas," in *Proc. IEEE-RAS 16th Int. Conf Humanoid Robots*, Nov. 2016, pp. 1312–1319, doi: 10.1109/HUMANOIDS.2016.7803439.

[7] M. Soni and R. Dahiya, "Soft eSkin: Distributed touch sensing with harmonized energy and computing," *Phil. Trans. Roy. Soc. A, Math., Phys. Eng. Sci.*, vol. 378, no. 2164, Feb. 2020, Art. no. 20190156, doi: 10.1098/rsta.2019.0156.

[8] R. Ramalingame *et al.*, "Flexible piezoresistive sensor matrix based on a carbon nanotube PDMS composite for dynamic pressure distribution measurement," *J. Sensors Syst.*, vol. 8, no. 1, pp. 1–7, Jan. 2019, doi: 10.5194/jsss-8-1-2019.

[9] O. Ozioko, P. Karipoth, P. Escobedo, M. Ntagios, A. Pullanchiyodan, and R. Dahiya, "SensAct: The soft and squishy tactile sensor with integrated flexible actuator," *Adv. Intell. Syst.*, vol. 3, no. 3, Mar. 2021, Art. no. 1900145, doi: 10.1002/aisy.201900145.

[10] A. H. A. Razak, A. Zayegh, R. K. Begg, and Y. Wahab, "Foot plantar pressure measurement system: A review," *Sensors*, vol. 12, no. 7, pp. 9884–9912, 2012.

[11] P. Escobedo, M. Ntagios, D. Shakthivel, W. T. Navaraj, and R. Dahiya, "Energy generating electronic skin with intrinsic tactile sensing without touch sensors," *IEEE Trans. Robot.*, vol. 37, no. 2, pp. 683–690, Apr. 2021, doi: 10.1109/TRO.2020.3031264.

[12] R. S. Dahiya, P. Mittendorfer, M. Valle, G. Cheng, and V. J. Lumelsky, "Directions toward effective utilization of tactile skin: A review," *IEEE Sensors J.*, vol. 13, no. 11, pp. 4121–4138, Nov. 2013, doi: 10.1109/JSEN.2013.2279056.

[13] S. Luo, J. Bimbo, R. Dahiya, and H. Liu, "Robotic tactile perception of object properties: A review," *Mechatronics*, vol. 48, pp. 54–67, Dec. 2017, doi: 10.1016/j.mechatronics.2017.11.002.

[14] Y. Huang, X. Fan, S. Chen, and N. Zhao, "Emerging technologies of flexible pressure sensors: Materials, modeling, devices, and manufacturing," *Adv. Funct. Mater.*, vol. 29, no. 12, Mar. 2019, Art. no. 1808509.

[15] M. Soni, M. Bhattacharjee, M. Ntagios, and R. Dahiya, "Printed temperature sensor based on PEDOT: PSS-graphene oxide composite," *IEEE Sensors J.*, vol. 20, no. 14, pp. 7525–7531, Jul. 2020, doi: 10.1109/JSEN.2020.2969667.

[16] S. Tsuji and T. Kohama, "Proximity skin sensor using time-of-flight sensor for human collaborative robot," *IEEE Sensors J.*, vol. 19, no. 14, pp. 5859–5864, Jul. 2019, doi: 10.1109/JSEN.2019.2905848.

[17] S. Gong *et al.*, "Highly stretchy black gold E-skin nanopatches as highly sensitive wearable biomedical sensors," *Adv. Electron. Mater.*, vol. 1, no. 4, Apr. 2015, Art. no. 1400063.

[18] B. Wang and A. Facchetti, "Mechanically flexible conductors for stretchable and wearable E-skin and E-textile devices," *Adv. Mater.*, vol. 31, no. 28, Jul. 2019, Art. no. 1901408.

[19] J. Wu *et al.*, "Highly flexible and sensitive wearable E-skin based on graphite nanoplatelet and polyurethane nanocomposite films in mass industry production available," *ACS Appl. Mater. Interfaces*, vol. 9, no. 44, pp. 38745–38754, Nov. 2017.

[20] R. S. Dahiya and M. Valle, *Robotic Tactile Sensing: Technologies and System*. Dordrecht, The Netherlands: Springer, 2013.

[21] G. Li, T. Liu, and J. Yi, "Wearable sensor system for detecting gait parameters of abnormal gaits: A feasibility study," *IEEE Sensors J.*, vol. 18, no. 10, pp. 4234–4241, May 2018, doi: 10.1109/JSEN.2018.2814994.

[22] I. González, J. Fontecha, R. Hervás, and J. Bravo, "An ambulatory system for gait monitoring based on wireless sensorized insoles," *Sensors*, vol. 15, no. 7, pp. 16589–16613, Jul. 2015, doi: 10.3390/s150716589.

[23] S. L. Patil, M. A. Thatte, and U. M. Chaskar, "Development of planter foot pressure distribution system using Flexi force sensors," *Sensors Transducers*, vol. 108, no. 9, pp. 73–79, Sep. 2009.

[24] M. Amjadi, M. Seong Kim, and I. Park, "Flexible and sensitive foot pad for sole distributed force detection," in *Proc. 14th IEEE Int. Conf. Nanotechnol.*, Aug. 2014, pp. 764–767, doi: 10.1109/NANO.2014.6968034.

[25] L.-M. Faller, C. Stetco, T. Mitterer, and H. Zangl, "An all-flexible sensing sole for legged robots," in *Proc. IEEE Int. Conf. Flexible Printable Sensors Syst. (FLEPS)*, Jul. 2019, pp. 1–3, doi: 10.1109/FLEPS.2019.8792287.

[26] L. Shu, T. Hua, Y. Wang, Q. Li, D. D. Feng, and X. Tao, "In-shoe plantar pressure measurement and analysis system based on fabric pressure sensing array," *IEEE Trans. Inf. Technol. Biomed.*, vol. 14, no. 3, pp. 767–775, May 2010, doi: 10.1109/TITB.2009.2038904.

[27] S. Crea, M. Donati, S. De Rossi, C. Oddo, and N. Vitiello, "A wireless flexible sensorized insole for gait analysis," *Sensors*, vol. 14, no. 1, pp. 1073–1093, Jan. 2014, doi: 10.3390/s140101073.

[28] S. Muzaffar and I. A. M. Elfadel, "Piezoresistive sensor array design for shoe-integrated continuous body weight and gait measurement," in *Proc. Symp. Design, Test, Integr. Packag. MEMS MOEMS (DTIP)*, May 2019, pp. 1–4, doi: 10.1109/DTIP.2019.8752629.

[29] A. M. Tan, F. K. Fuss, Y. Weizman, and O. Troynikov, "Development of a smart insole for medical and sports purposes," *Proc. Eng.*, vol. 112, pp. 152–156, Jan. 2015, doi: 10.1016/j.proeng.2015.07.191.

[30] Z. Lin *et al.*, "A triboelectric nanogenerator-based smart insole for multifunctional gait monitoring," *Adv. Mater. Technol.*, vol. 4, no. 2, Feb. 2019, Art. no. 1800360, doi: 10.1002/admt.201800360.

[31] J. Wheeler *et al.*, "In-sole MEMS pressure sensing for a low-erextremity exoskeleton," in *Proc. 1st IEEE/RAS-EMBS Int. Conf. Biomed. Robot. Biomechatronics, BioRob.*, 2006, pp. 31–34, doi: 10.1109/BIOROB.2006.1639055.

[32] C. Deng, W. Tang, L. Liu, B. Chen, M. Li, and Z. L. Wang, "Self-powered insole plantar pressure mapping system," *Adv. Funct. Mater.*, vol. 28, no. 29, Jul. 2018, Art. no. 1801606, doi: 10.1002/adfm.201801606.

[33] C. Wang, Y. Kim, H. Shin, and S. D. Min, "Preliminary clinical application of textile insole sensor for hemiparetic gait pattern analysis," *Sensors*, vol. 19, no. 18, p. 3950, Sep. 2019, doi: 10.3390/s19183950.

[34] S. W. Park, P. S. Das, and J. Y. Park, "Development of wearable and flexible insole type capacitive pressure sensor for continuous gait signal analysis," *Organic Electron.*, vol. 53, pp. 213–220, Feb. 2018, doi: 10.1016/j.orgel.2017.11.033.

[35] E. Macdonald *et al.*, "3D printing for the rapid prototyping of structural electronics," *IEEE Access*, vol. 2, pp. 234–242, 2014, doi: 10.1109/ACCESS.2014.2311810.

[36] M. Ntagios, S. Dervin, and R. Dahiya, "3D printed capacitive pressure sensing sole for anthropomorphic robots," in *IEEE Int. Conf. Flexible Printable Sensors Syst. (FLEPS)*, 2021, pp. 1–4, doi: 10.1109/FLEPS51544.2021.9469839.

[37] M. Ntagios, P. Escobedo, and R. Dahiya, "3D printed robotic hand with embedded touch sensors," in *Proc. IEEE Int. Conf. Flexible Printable Sensors Syst. (FLEPS)*, Aug. 2020, pp. 1–4, doi: 10.1109/FLEPS49123.2020.9239587.

[38] H. Nassar and R. Dahiya, "Fused deposition modeling-based 3D-printed electrical interconnects and circuits," *Adv. Intell. Syst.*, vol. 3, no. 12, Dec. 2021, Art. no. 2100102.

[39] M. Ntagios, H. Nassar, A. Pullanchiyodan, W. T. Navaraj, and R. Dahiya, "Robotic hands with intrinsic tactile sensing via 3D printed soft pressure sensors," *Adv. Intell. Syst.*, vol. 2, no. 6, Jun. 2020, Art. no. 1900080, doi: 10.1002/aisy.201900080.

[40] M. Sakin and Y. C. Kiroglu, "3D printing of buildings: Construction of the sustainable houses of the future by BIM," *Energy Proc.*, vol. 134, pp. 702–711, Oct. 2017.

[41] C. R. Garcia, R. C. Rumpf, H. H. Tsang, and J. H. Barton, "Effects of extreme surface roughness on 3D printed horn antenna," *Electron. Lett.*, vol. 49, no. 12, pp. 734–736, 2013.

[42] A.-V. Do, B. Khorsand, S. M. Geary, and A. K. Salem, "3D printing of scaffolds for tissue regeneration applications," *Adv. Healthcare Mater.*, vol. 4, no. 12, pp. 1742–1762, Aug. 2015.

[43] S. Bukhari, B. J. Goodacre, A. AlHelal, M. T. Kattadiyil, and P. M. Richardson, "Three-dimensional printing in contemporary fixed prosthodontics: A technique article," *J. Prosthetic Dentistry*, vol. 119, no. 4, pp. 530–534, Apr. 2018, doi: 10.1016/j.prosdent.2017.07.008.

[44] A. Liu *et al.*, "3D printing surgical implants at the clinic: A experimental study on anterior cruciate ligament reconstruction," *Sci. Rep.*, vol. 6, no. 1, pp. 1–13, Apr. 2016.

[45] A. Christou, M. Ntagios, A. Hart, and R. Dahiya, "GlasVent—The rapidly deployable emergency ventilator," *Global Challenges*, vol. 4, no. 12, Dec. 2020, Art. no. 2000046.

[46] M. I. U. Haq *et al.*, "3D printing for development of medical equipment amidst coronavirus (COVID-19) pandemic—Review and advancements," *Res. Biomed. Eng.*, vol. 38, pp. 1–11, Oct. 2020.

[47] M. Despeisse *et al.*, "Unlocking value for a circular economy through 3D printing: A research agenda," *Technol. Forecasting Social Change*, vol. 115, pp. 75–84, Feb. 2017.

[48] T.-C. Hou, Y. Yang, H. Zhang, J. Chen, L.-J. Chen, and Z. L. Wang, "Triboelectric nanogenerator built inside shoe insole for harvesting walking energy," *Nano Energy*, vol. 2, no. 5, pp. 856–862, Sep. 2013, doi: 10.1016/j.nanoen.2013.03.001.

[49] Q. Zhang, Y. L. Wang, Y. Xia, X. Wu, T. V. Kirk, and X. D. Chen, "A low-cost and highly integrated sensing insole for plantar pressure measurement," *Sens. Bio-Sens. Res.*, vol. 26, Nov. 2019, Art. no. 100298, doi: 10.1016/j.sbsr.2019.100298.

[50] M. O. Shaikh, Y.-B. Huang, C.-C. Wang, and C.-H. Chuang, "Wearable woven triboelectric nanogenerator utilizing electrospun PVDF nanofibers for mechanical energy harvesting," *Micromachines*, vol. 10, no. 7, p. 438, Jun. 2019, doi: 10.3390/mi10070438.

[51] D. P. J. Cotton, I. M. Graz, and S. P. Lacour, "A multifunctional capacitive sensor for stretchable electronic skins," *IEEE Sensors J.*, vol. 9, no. 12, pp. 2008–2009, Dec. 2009, doi: 10.1109/JSEN.2009.2030709.
[52] S.-J. Woo, J.-H. Kong, D.-G. Kim, and J.-M. Kim, "A thin all-elastomeric capacitive pressure sensor array based on micro-contact printed elastic conductors," *J. Mater. Chem. C*, vol. 2, no. 22, pp. 4415–4422, 2014.
[53] M. Ying *et al.*, "Silicon nanomembranes for fingertip electronics," *Nanotechnology*, vol. 23, no. 34, Aug. 2012, Art. no. 344004, doi: 10.1088/0957-4484/23/34/344004.

M. Ntagios (Member, IEEE) received the B.Eng. (Hons.) degree in electronic engineering from the University of Bedfordshire, Luton, U.K., in 2017. He is currently pursuing the Ph.D. degree with the Bendable Electronics and Sensing Technologies (BEST) Group, James Watt School of Engineering, University of Glasgow, Glasgow, U.K.

Ravinder Dahiya (Fellow, IEEE) is currently a Professor of Electronics and Nanoengineering with the University of Glasgow, U.K. He is also the Leader of the Bendable Electronics and Sensing Technologies (BEST) Research Group. His group conducts fundamental and applied research in the multidisciplinary fields of flexible and printable electronics, tactile sensing, electronic skin, robotics, and wearable systems. He has authored or coauthored more than 400 publications, books, and submitted/granted patents and disclosures. He has led several international projects. He has received the Prestigious EPSRC Fellowship, the Marie Curie Fellowship, and the Japanese Monbusho Fellowship. He is a Fellow of the Royal Society of Edinburgh. He has received several awards, including 11 best journals/conference paper awards as the author/coauthor, 2016 Microelectronic Engineering Young Investigator Award, and the 2016 Technical Achievement Award from the IEEE Sensors Council. He has been the general chair and the technical program chair of several conferences. He is the President of IEEE Sensors Council and the Founding Editor-in-Chief of IEEE JOURNAL ON FLEXIBLE ELECTRONICS (J-FLEX). He has served on the editorial boards of *Scientific Reports*, IEEE SENSORS JOURNAL, and the IEEE TRANSACTIONS ON ROBOTICS. He was a Distinguished Lecturer of IEEE Sensors Council from 2016 to 2021.